Imprint of charge and oxygen orders on Dy ions in $DyBa_2Cu_3O_{6+x}$ thin films probed by resonant x-ray scattering

Davide Betto,[1,*] Martin Bluschke,[1,2] Daniel Putzky,[1] Enrico Schierle,[2] Andrea Amorese,[3] Katrin Fürsich,[1] Santiago Blanco-Canosa,[4,5] Georg Christiani,[1] Gennady Logvenov,[1] Bernhard Keimer,[1] and Matteo Minola[1,†]

[1]*Max Planck Institute for Solid State Research, Heisenbergstraße 1, D-70569 Stuttgart, Germany*
[2]*Helmholtz-Zentrum Berlin für Materialien und Energie, Albert-Einstein-Straße 15, D-12489 Berlin, Germany*
[3]*Max Planck Institute for Chemical Physics of Solids, Nöthnitzer Straße 40, D-01187 Dresden, Germany*
[4]*Donostia International Physics Center, DIPC, E-20018 Donostia-San Sebastian, Basque Country, Spain*
[5]*IKERBASQUE, Basque Foundation for Science, E-48013 Bilbao, Basque Country, Spain*

(Received 11 September 2020; revised 10 November 2020; accepted 10 November 2020; published 30 November 2020)

We used resonant x-ray scattering at the Cu L_3 and Dy M_5 edges to investigate charge order in thin films of underdoped $DyBa_2Cu_3O_{6+x}$ (DyBCO) epitaxially grown on $NdGaO_3$ (110) substrates. The films show an orthorhombic crystal structure with short-range ortho-II oxygen order in the charge-reservoir layers. At the Dy M_5 edge we observe diffraction peaks with the same planar wave vectors as those of the two-dimensional charge density wave in the CuO_2 planes and of the ortho-II oxygen order, indicating the formation of induced ordered states on the rare-earth sublattice. The intensity of the resonant diffraction peaks exhibits a nonmonotonic dependence on an external magnetic field. Model calculations on the modulation of the crystalline electric field at the Dy sites by charge and oxygen order capture the salient features of the magnetic field, temperature, and photon energy dependence of the scattering intensity.

DOI: 10.1103/PhysRevB.102.195149

I. INTRODUCTION

Strongly correlated compounds are often characterized by a great variety of phases which are frequently in competition with each other. The high-temperature superconducting cuprates represent a particularly interesting case given the richness of their phase diagram, with antiferromagnetism, superconductivity, electronic nematicity, and charge order in close proximity of one another [1]. In this work, we investigated the charge ordered state in $DyBa_2Cu_3O_{6+x}$ (DyBCO) thin films using resonant x-ray scattering (RXS). The "123" family of cuprates $RBa_2Cu_3O_{6+x}$ (RBCO), where R is a rare-earth, is best known for the compound YBCO, which has been extensively investigated in recent years, owing to its high superconducting critical temperature (T_c) and very low chemical disorder. In addition to the superconducting CuO_2 planes, the crystal structure of these materials comprises a charge-reservoir layer with CuO chains. Hole doping of the CuO_2 plane can be achieved with relatively little associated disorder by introducing additional oxygen ions into the charge-reservoir layer. In underdoped YBCO, the CuO chains run along the b direction and organize in regular sequences of filled and empty sites along the a direction, resulting in a uniaxial superstructure (termed ortho-ordering) whose spatial period depends on the doping [2].

RXS at the Cu L_3 edge has proven to be an efficient method of investigating charge density wave (CDW) order because it is sensitive enough to detect short-range correlations and CDW fluctuations. In underdoped YBCO, charge order diffraction peaks have been observed along both planar bond directions [3], and have been interpreted in terms of perpendicular domains of uniaxial CDW correlations [4,5]. At zero magnetic field, and in the absence of external pressures, this charge order is confined to the CuO_2 planes, with little correlation along the c direction [6]. The temperature dependence of the CDW diffraction peaks in YBCO shows a maximum in the scattering intensity for $T = T_c$. At the same temperature, the correlation length ξ reaches a maximum of $\sim$20 lattice parameters [7]. This behavior implies a strong competition between charge order and superconductivity in YBCO. The incident photon energy dependence of the CDW peaks also clearly shows that the Cu ions in the CuO_2 planes (with a valence state close to Cu^{2+}) take part in the charge ordering phenomena, while the Cu^{1+} atoms in the charge-reservoir layers are not involved. The converse is true for the ortho-order peaks. The Y^{3+} ions (with a full-shell electron configuration) do not participate in the charge ordering.

In addition to the quasi-two-dimensional (quasi-2D) CDW and superconductivity, several recent studies have demonstrated that a long-range three-dimensional (3D) charge ordered state can be stabilized in underdoped YBCO by the application of various external fields [8]. This 3D CDW

*d.betto@fkf.mpg.de
†m.minola@fkf.mpg.de

Published by the American Physical Society under the terms of the Creative Commons Attribution 4.0 International license. Further distribution of this work must maintain attribution to the author(s) and the published article's title, journal citation, and DOI. Open access publication funded by the Max Planck Society.

manifests itself as a sharp diffraction peak at integer values of the out-of-plane Miller index L, and appears to coexist with the 2D CDW, whose diffraction signatures remain intact across the 3D CDW transition. First, it was found that by applying high external magnetic fields along the c axis [9,10] ($\geqslant$15 T), the 3D CDW forms only along the b axis, in concomitance with the suppression of superconductivity. More recently, it has been shown that a similar 3D charge order can also be induced in YBCO crystals by uniaxial strain along the a axis [5,11] and by epitaxial growth of thin films on cubic $SrTiO_3$ (STO) substrates [12]. In all cases, the 3D CDW shares the same in-plane wave vector with its 2D counterpart. In contrast to the case of bulk YBCO, epitaxially induced 3D CDW correlations are extraordinarily robust, demonstrating little or no suppression upon entering the superconducting phase and surviving up to and above room temperature. These findings point towards a structural mechanism stabilizing the 3D CDW in YBCO thin films. An independent study on the related "123" cuprate material $(Ca_xLa_{1-x})(Ba_{1.75-x}La_{0.25+x})Cu_3O_y$ (CLBLCO) showed that structural degrees of freedom couple strongly to the 2D CDW as isovalent chemical substitution on the A and B sites was used to redistribute chemical pressure within the unit cell [13].

RBCO compounds with $R \neq$ Y differ from YBCO in two respects. First, the different sizes of the R^{3+} ions modify the interatomic distances and associated electronic hopping parameters, resulting in slight variations of the electronic properties, including the superconducting T_c. Second, the partially filled f shells generate magnetic moments that are, however, only weakly coupled to the conduction electrons in the CuO_2 planes. (Note that the $R =$ Pr compound is anomalous because of deviations from the 3+ valence state and/or hybridization of Pr orbitals with electronic states in the CuO_2 planes [14].)

To investigate the impact of these effects on CDW order, we have performed RXS experiments on DyBCO thin films synthesized by molecular beam epitaxy [15]. The electronic properties of the Dy^{3+} ions (electron configuration $4f^9$) in DyBCO have been studied in bulk DyBCO crystals by paramagnetic resonance and neutron scattering [16,17]. In the D_{2h} point group symmetry, the ground state is composed almost exclusively of the $M_J = \pm 11/2$ component of the $J = 15/2$ multiplet. The magnetic moments generated in this way interact weakly and order antiferromagnetically at 1 K [18]. Since the presence of ortho-order is known to modify the crystal field environment surrounding the Dy ions [19], we used Dy M-edge RXS to investigate possible imprints of CDW and oxygen order on the resonant diffraction cross section.

In our study of DyBCO thin films we have first used Cu L_3-edge RXS to detect a 2D CDW that resonates with the Cu^{2+} ions of the CuO_2 planes, analogous to prior work on YBCO [20]. Surprisingly, we also observed an ortho-II CuO chain order in the charge reservoir layer, a phenomenon which has not previously been observed in cuprate thin films. When tuning the incident photon energy to the Dy M_5 resonance, diffraction peaks are observed at the wave vectors associated with both the CDW and the CuO chain order. The temperature, field, and photon energy dependence of these reflections are consistent with those of an induced ordering phenomenon. We also report the absence of 3D CDW correlations in our films and discuss the possible role of structural degrees of freedom in suppressing the 3D ordered state.

II. EXPERIMENTAL DETAILS

The thin films of DyBCO were grown on orthorhombic $NdGaO_3$ (NGO) (110) substrates using layer-by-layer molecular beam epitaxy, which produces films with the c axis perpendicular to the surface. The crystalline quality was characterized by x-ray diffraction and scanning transmission electron microscopy, while T_c was obtained by mutual inductance measurements. We measured two films, both 20 u.c. thick. Both samples were reduced after growth resulting in $T_c \sim 55(5)$ K, which corresponds to approximately $x = 0.5$ in bulk crystals. However, repeated characterization of the superconducting critical temperature revealed a further decrease in the oxygen content over a time scale of days and weeks. Nevertheless, the presence of both ortho-II and CDW ordering reflections in our RXS experiments verify that the doping level of our samples remained in the underdoped regime during the measurements presented here. We observed no sign of changes due to beam damage. The films show orthorhombic twin domains as previously reported [21], thereby making the two in-plane directions equivalent in our measurements, which average over a $\sim$200 μm beam spot. Details of the growth and characterization are given in Ref. [15] and in Supplemental Material [22].

The x-ray measurements were performed at the UE46 PGM-1 beamline of the Helmholtz-Zentrum Berlin at BESSY-II. The experimental station comprises two different ultra-high-vacuum chambers, one of which allows for the application of an external magnetic field up to 6 T using an in-vacuum rotatable superconducting coil. The rotation of this coil, and therefore the field direction, is limited to a set of angular ranges for which the coil does not interfere with the x-ray beam path. For the RXS measurements of the CDW at the Dy M_5 edge, the applied field was kept at $\sim$45° from the in-plane direction in the a-c plane [angle α in Fig. 1(b)], which is the lowest angle allowed by the geometry. For the ortho-order measurement at the same edge, the field was directed at $\alpha \sim 30°$. The liquid helium cryostat produces a sample environment with temperatures as low as 5 K. The incoming light polarization was either parallel (π) or perpendicular (σ) to the horizontal scattering plane.

RXS is a photon-in-photon-out technique where the scattering signal is greatly enhanced by tuning the incoming energy to a particular absorption edge of an ion in the compound. When the incident photon energy is tuned to an absorption edge, the photon energy satisfies a resonance condition which strongly couples a core electronic state to the valence states during the scattering process. RXS is therefore sensitive to variations in the charge and/or magnetic degrees of freedom in the valence electrons of the scattering ions. In RBCO compounds, there are two inequivalent Cu ions in the structure, one in the CuO_2 planes (approximately Cu^{2+}) and one in the chains (approximately Cu^{1+}), with the exact valence states depending on the doping level. These distinct sites give rise to specific features in the absorption spectra at the Cu L_3 resonance ($\sim$931 eV) [23]. Accordingly, measuring the diffraction peak's incident photon energy dependence in the

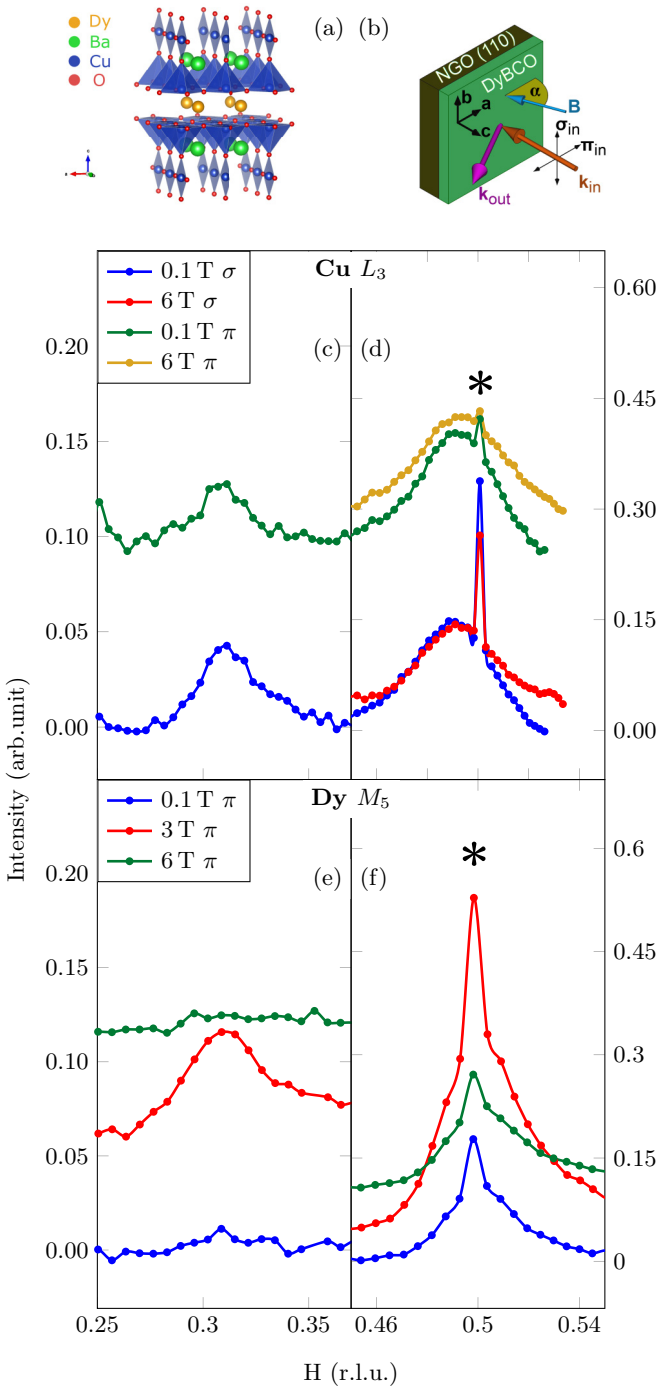

FIG. 1. (a) DyBCO crystal structure. (b) Sketch of the experimental scattering geometry. (c)–(f) Rocking scans (converted to reciprocal-space coordinate H) for DyBCO at the Cu L_3 (c) and (d) and Dy M_5 (e) and (f) edges [around 932 eV for (c) and (d), and 1294 eV for (e) and (f)] at different magnetic field values. The curves have been shifted vertically [by multiples of 0.05 in (c), 0.2 in (d), and 0.06 in (e) and (f)] for clarity. The spikes marked by asterisks in (d) and (f) at exactly $q = (0.5, 0.0)$ arise from the substrate and should therefore be ignored. During the scans the L value varies in the range (0.6–1.6) and (1.65–2.4) for Cu and Dy edges, respectively.

vicinity of an absorption edge allows us to determine which electronic states, and thus which ions, are involved in the diffracting superstructure. In addition, at the Dy M_5 resonance

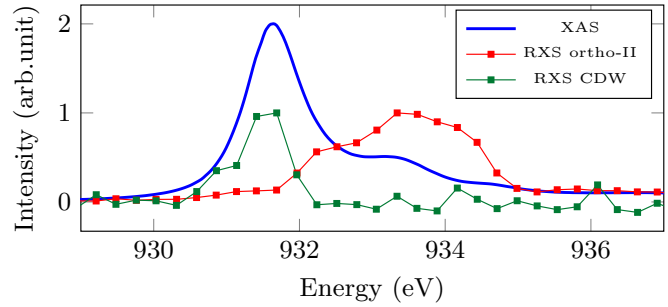

FIG. 2. Cu L_3 incident photon energy dependence of the RXS reflections at $q = (0.5, 0.0, 0.835)$ and $(0.315, 0.0, 1.45)$. The spectra were taken at 5 K with σ polarization of the x rays and no external magnetic field.

(1292 eV) it is also possible to determine if a diffraction peak originates from orbital or magnetic ordering by considering the detailed RXS spectroscopic lineshape [24]. The x-ray absorption spectra (XAS) consists of three peaks at ∼1290, 1292, and 1294 eV, which we label A, B, and C (see Fig. 4). Peaks A and C correspond to $\Delta J = \pm 1$ transitions, while peak B corresponds to $\Delta J = 0$ transitions. Each J level is also split into M_J levels by the crystal field or by applied magnetic fields, with the additional selection rule $\Delta M_J = 0, \pm 1$ applying to electric-dipole-allowed transitions. In magnetically ordered systems, each ΔJ transition in Dy ions is dominated by a single ΔM_J value and therefore the latter selection rule approximates that of ΔJ [25]. In first approximation, in a resonant absorption process, intensity at peaks A and C corresponds to electronic transitions of magnetic nature, while peak B corresponds to a transition of orbital origin [26]. In the scattering profile, following Kramers-Kronig relations, a dominant intensity at peak B is thus a clear fingerprint of orbital scattering, while structural and magnetic scattering results in a broader intensity distribution with a clear maximum at peak C [24].

III. RESULTS

Figure 1 shows rocking scans projected onto the [10] direction of the DyBCO thin films at both the Cu L_3 and Dy M_5 edges for increasing external magnetic fields. The scans at the Cu edge show a CDW peak at $q \sim (0.315, 0.0)$, as expected, and, remarkably, also a broad ortho-II peak close to $q = (0.5, 0.0)$. Throughout this manuscript we will refer to positions in the 2D reciprocal space (H, K) in units of $(2\pi/a, 2\pi/b)$ (reciprocal lattice units, r.l.u.) with a and b the in-plane lattice parameters. The incident photon energy dependence of the peak intensities is shown in Fig. 2. Each peak exhibits a characteristic resonance profile. The CDW, associated with the Cu^{2+} ions of the CuO_2 planes, is peaked near 931.7 eV. In contrast, the ortho-II CuO chain order reflection is associated with copper ions in the charge reservoir layer and peaks at higher energies near 933.2 eV. Contrary to similar YBCO thin films grown on STO [12], no signature of a 3D CDW was found (see Supplemental Material [22]). While it has been shown that *R*BCO compounds can grow in the orthorhombic structure in thin film form [15,21], the presence of ortho-order CuO chains is remarkable since these have not been reported in *R*BCO thin films to date.

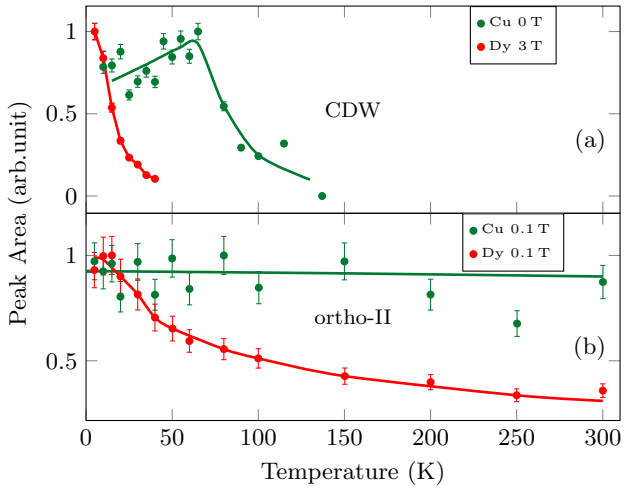

FIG. 3. Temperature dependence of the charge order (a) and ortho-order (b) peaks. Data for Cu and Dy was taken at 931.6 eV and 1294 eV, respectively. The maximum intensity of each data set is normalized to 1. Lines are guides to the eye.

The most interesting result, however, is found when the incident photon energy is tuned to the Dy M_5 edge. Both the CDW and the ortho-II order peaks are detected on the Dy sublattice, with maximum intensity around 2–3 T, indicating that the modulation in the Cu atoms is transferred to the Dy ions. The correlation lengths at 5 K are ∼27 Å and ∼32 Å for the induced ortho and CDW orders, respectively. In various transition metal oxides [27,28] and other multinary rare-earth containing systems, such as the rare-earth tritellurides [29] or synthetic multilayer systems [30], the formation of induced

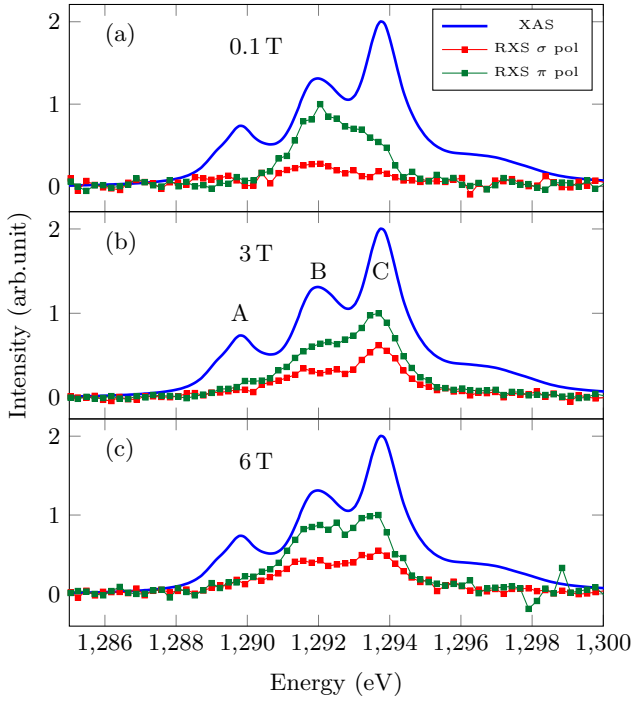

FIG. 4. Dy M_5 incident photon energy dependence of the RXS reflection at (0.5, 0.0, 1.89) for increasing magnetic field. The intensities of the XAS and the RXS spectra are normalized to 2 and 1 (for π polarization), respectively. All data was taken at 5 K.

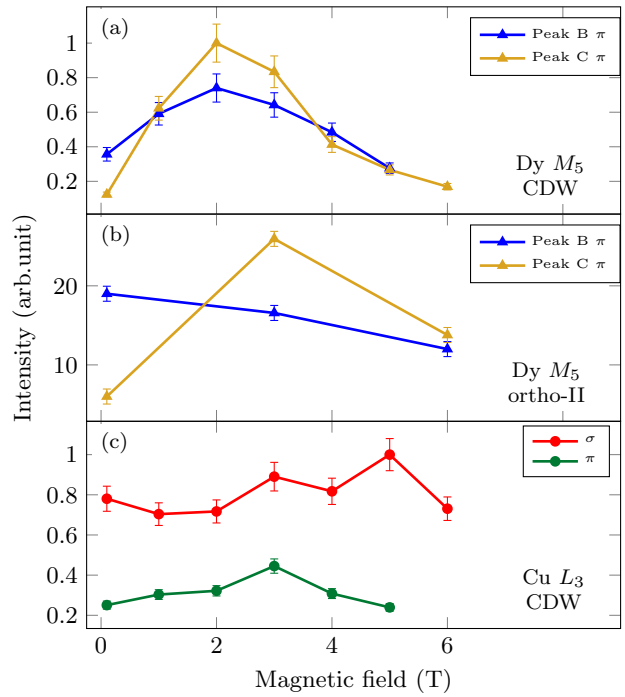

FIG. 5. Magnetic field dependence at the Dy M_5 edge of (a) the CDW induced peak and (b) the ortho-II induced peak; (c) the CDW peak at the Cu L_3 edge. Peak C of the XAS (energy 1294 eV) is of magnetic origin, while peak B (energy 1292 eV) is of charge, orbital, or structural origin [24]. The magnetic field was applied at an angle $\alpha \sim 45^\circ$ for the Dy CDW induced peak in (a), at $\alpha \sim 30^\circ$ for the ortho-II induced peak in (b), and at $\alpha \sim 45^\circ$ for the Cu CDW peak in (c). See Fig. 1(b) for a sketch of the experimental scattering geometry. All data was taken at 5 K.

order on the rare-earth sublattice has already been observed. Likewise, in DyBCO, the temperature-dependent resonant scattering intensity at the Dy edge decays quickly with temperature, reflecting the temperature-dependent susceptibility of the Dy sublattice [Fig. 3(a)]. This is in contrast to the behavior of the two corresponding reflections measured at the Cu L_3 edge, where the CDW peak decreases rapidly in intensity only above the superconducting transition [20] and the ortho-order peak is almost constant up to room temperature [Fig. 3(b)], in agreement with prior work on bulk single crystals [20].

The photon energy dependence of the ortho-II induced peak at the Dy M_5 edge is shown in Fig. 4 for different magnetic fields. Figure 5(b) demonstrates that the resonance at energies corresponding to peak C of the XAS has a nonmonotonic field dependence, with its maximum occurring near 3 T.

We now turn our attention to the charge order induced peak at $q = (0.315, 0.0)$ measured at the Dy M_5 edge (see Fig. 6 for the field dependence plot). At low fields (0.1 T), the energy dependence of the reflection, shown in Fig. 7(c), demonstrates essentially no scattering at photon energies corresponding to peak C, while some intensity is visible at peak B, indicating some orbital origin. However, it should be noted that the overall signal is weakest at low fields, possibly hampering our ability to accurately determine the resonant line shape. At higher fields, the contribution of peak C becomes dominant, indicating enhanced magnetic scattering [31]. The total

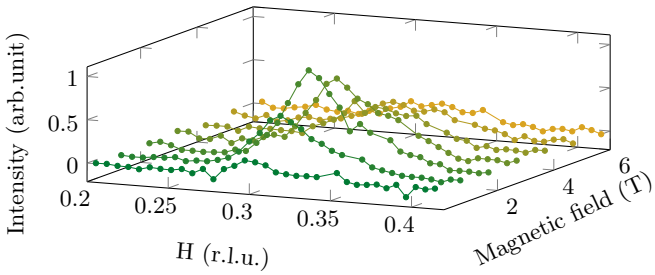

FIG. 6. Magnetic field dependence of the charge order induced peak at the Dy M_5 edge (1294 eV), taken at 5 K and with π polarization of the incoming light. Scans have been measured around $q = (0.315, 0.0, 2.24)$. The data is normalized to 1.

intensity peaks around 2–3 T and is suppressed again at higher fields [see Fig. 5(a)]. Therefore, our data clearly indicates that this induced order has an important contribution of magnetic origin, as implied by the strong field dependence and the maximum at peak C. A similar dependence of the RXS signal on the field strength has been observed by Donnerer *et al.* [28] in $Tb_2Ir_2O_7$. Finally, we observed that modifying the field direction from $\alpha \sim 45°$ towards a fully out-of-plane configuration, i.e., along the c axis, severely reduces the scattering signal [Fig. 7(b)].

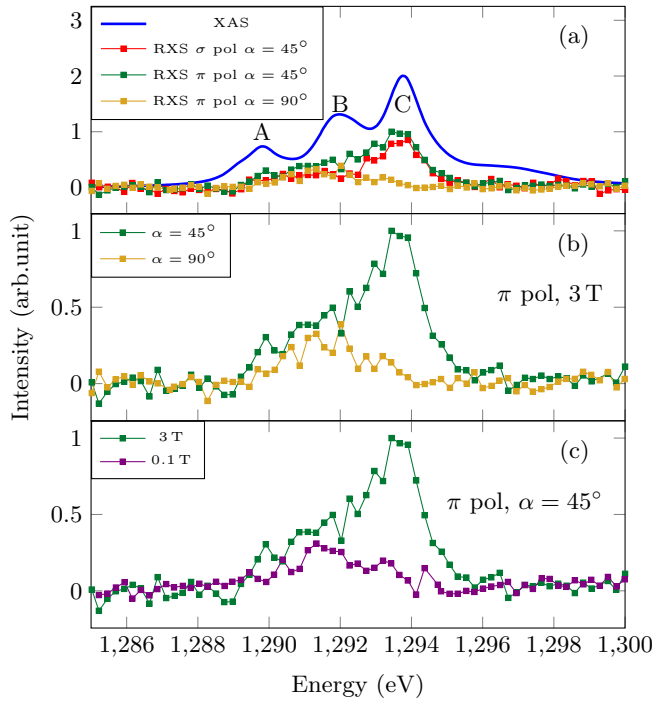

FIG. 7. (a) Dy M_5 incident photon energy dependence of the RXS reflection at the CDW $q = (0.315, 0.0, 2.24)$. All data in this panel was taken at 3 T but it is representative for field values $1-6T$: The intensity changes with field but the spectral shape does not. The intensities of the XAS and the RXS spectra have each been scaled in order to facilitate a comparison of their lineshapes. (b) Comparison between the RXS signal for different α values. (c) Comparison between the RXS signal at high and low magnetic field. All data was taken at 5 K.

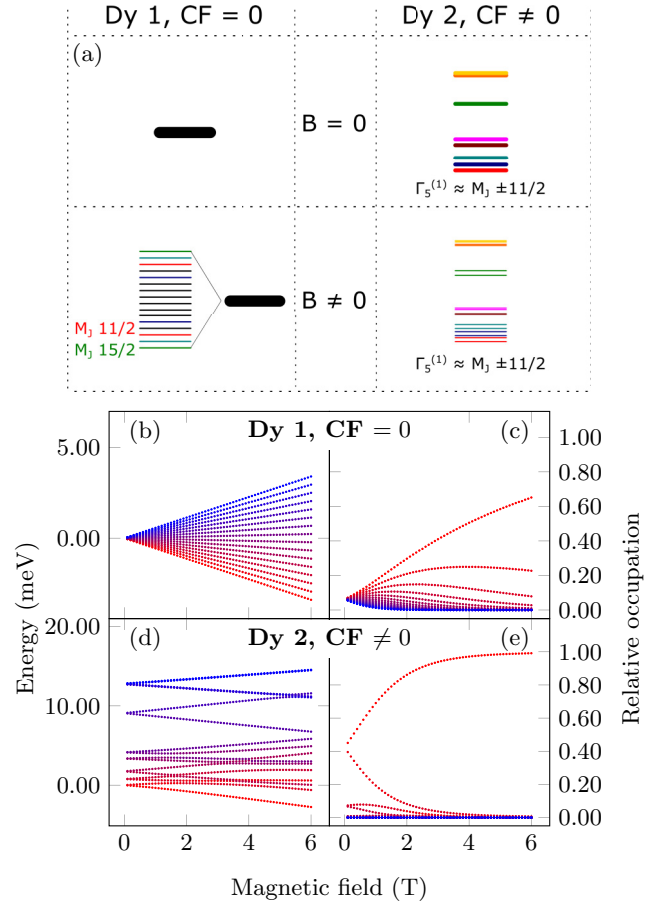

FIG. 8. (a) Sketch of the Dy electronic levels for the two different sites [with and without crystal field (CF) and external magnetic field]. The crystal field and the magnetic field tend to stabilize different electronic levels as ground states. It is worth noticing that the Γ multiplets only roughly correspond to the M_J states [17]. (b) Energy levels for a Dy ion without crystal field (Dy 1) as a function of the applied magnetic field at $\alpha = 45°$. (c) Boltzmann occupation of the levels in (b) at 5 K. (d) Energy levels for a Dy ion with crystal field (Dy 2) as a function of the applied magnetic field at $\alpha = 45°$. (e) Boltzmann occupation of the levels in (d) at 5 K.

IV. DISCUSSION

Our RXS study of DyBCO films shows a 2D CDW in the CuO_2 planes without any evidence for long-range correlations along the c direction (i.e., no 3D CDW). These findings are analogous to bulk YBCO but differ from a related report on YBCO films grown on $SrTiO_3$, for which a 3D CDW was observed in zero field [12]. In Ref. [12] it is argued that the suppression of orthorhombic crystal symmetry, via the epitaxial relationship to the cubic substrate, may promote 3D CDW correlations in the YBCO thin films. According to this picture the bulklike CuO chain order and associated orthorhombic crystal symmetry of our DyBCO films may be responsible for inhibiting the formation of a 3D CDW. However, other degrees of freedom are manipulated upon substitution of Y for Dy. Not least among these is the presence of a large $4f$ moment on the Dy site, which we have shown is coupled to the CDW. Additionally, small variations in bond angles and lengths associated with the smaller size of the Dy ion

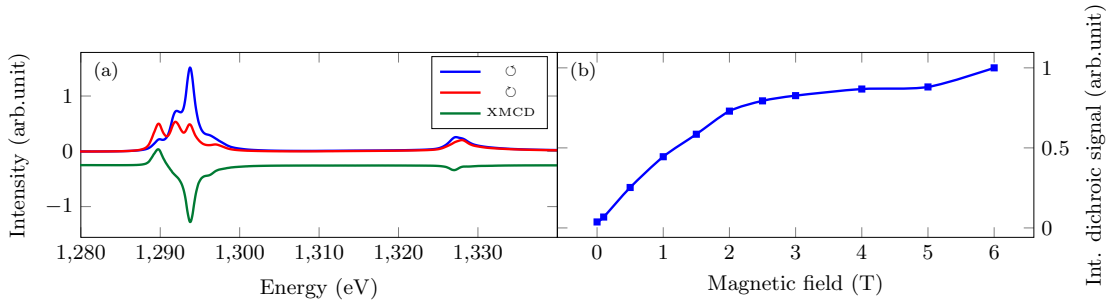

FIG. 9. XAS and XMCD spectra at 6 T (a) and field dependence of the integrated dichroic signal (b). The XMCD curve in (a) has been shifted downwards by 0.25 for clarity. The data was taken at 5 K.

may have important implications for the charge ordered state, similar to the structural modifications achieved in CLBLCO upon isovalent chemical substitution [13]. Further work is required to elucidate the full impact of epitaxial growth and structural degrees of freedom on the charge ordered state in cuprates.

Our magnetic field-dependent measurements clearly suggest that the magnetic moment of the Dy ions must play a crucial role in coupling the rare-earth sublattice to the electronic and structural degrees of freedom in CuO_2 planes and in the charge-reservoir layer. Lee *et al.* [29] described the formation of an induced charge order on the rare-earth atoms in tritellurides as a periodic modulation of the crystal field acting on the different M_J levels of the spin-orbit coupled electronic ground state. We performed calculations akin to the ones in Lee *et al.* [29] using the QUANTY code [32]. The scattering tensor for a Dy^{3+} ion in a D_{2h} crystal field (according to Ref. [17]) is calculated for different magnetic field values. Slater integrals and spin-orbit coupling parameters are calculated using Cowan's code [33]. Boltzmann averaging is performed to obtain the thermal occupation of the lowest energy states.

As the CDW is incommensurate and involves motion of multiple ions in the unit cell, accurate modeling of the corresponding crystalline electric field at the Dy site is a formidable task. To capture the essence of the mechanism underlying the imprint of CDW order on the Dy sublattice, we adopt a simple model with only two Dy sites, which can be thought of as those experiencing the maximum and minimum CDW-induced modulation. For simplicity, the crystal field acting on one of these ions is assumed to be identical to the one described by parameters extracted from neutron scattering experiments, apart from a rescaling factor of 0.25 [17], and the other one is assumed to be isotropic. The choice of this specific value is motivated by the goal of reproducing the measured field and temperature dependencies. Other rescaling factors were tried but resulted in worse agreement [34]. Note that RXS is sensitive only to the difference in the scattering tensors of the two ions, while inelastic neutron scattering is a direct probe of the CF splitting. In addition, the crystal field in thin-film structure may differ from the bulk, especially for ions near the surface and substrate interface. The modulation of the scattering tensor between these two sites is used to represent the periodic modulation of the crystal field parameters associated with the charge density wave (or ortho-order), and the resonant scattering profile is obtained by taking the difference of the scattering tensors at the two sites. The implemented Hamiltonian has the form,

$$\mathcal{H} = \sum_i \left(\frac{p_i^2}{2m} + \frac{-Ze^2}{r_i} + \xi(r_i) l_i \cdot s_i \right) + \sum_{i>j} \frac{e^2}{r_{ij}} - \sum_i eV_{\mathrm{CF}} + \sum_i \vec{J} \cdot \vec{B}.$$

In order from left to right, the terms are as follows: kinetic energy, nuclear potential, spin-orbit coupling, electron-electron interaction, crystal field potential, and Zeeman energy. As usual, the kinetic and nuclear one-electron terms are grouped in a general central potential. The electron-electron interaction is treated in terms of Slater's integrals $\sum_i (f_i F^i + g_i G^i)$, while the crystal field potential is expanded into renormalized spherical harmonics $V_{\mathrm{CF}} = \sum_{k=0}^{\infty} \sum_{m=-k}^{+k} A_k^m r^k C_k^m$. The scattering tensor $F_{1,2}$ is then calculated for the two Dy ions and the RXS intensity at the modulation wave vector is proportional to $|F_1 - F_2|$ [35].

At one site the Dy crystal field parameters stabilize the $M_J = \pm 11/2$ ground state in zero field, whereas on the other site all M_J states are degenerate. An external magnetic field then splits all Kramer's doublets via the Zeeman effect resulting in an $M_J = 15/2$ ground state for sufficiently high fields, i.e., the state with the largest magnetic moment component along the field direction. For intermediate fields, both sites exhibit a net moment in the direction of the field, but the magnitude of the moments is modulated by the distinct crystal field environments at the two sites. Figure 8(a) shows a sketch of the resulting crystal-field eigenstates with and without magnetic field for the Dy ions at the two sites. The mechanism behind the peculiar nonmonotonic field dependence of the induced order is then captured by Figs. 8(b)–8(e), which show the calculated field dependence of the states and the corresponding Boltzmann occupation at 5 K for zero [Figs. 8(b) and 8(c)] and nonzero crystal field [Figs. 8(d) and 8(e)]. The RXS intensity results then from the contrast arising from the small changes in the level occupations and the XAS final state of the two Dy sites. Notice in particular in Fig. 8(d) the crossing of the low-lying energy levels around 2–3 T, which, in concert with the evolving level occupations, is likely responsible for the maximum at the same field value of the RXS signal measured on peak C [Fig. 5(a)]. In the real material we believe that the magnetic component of the resonant

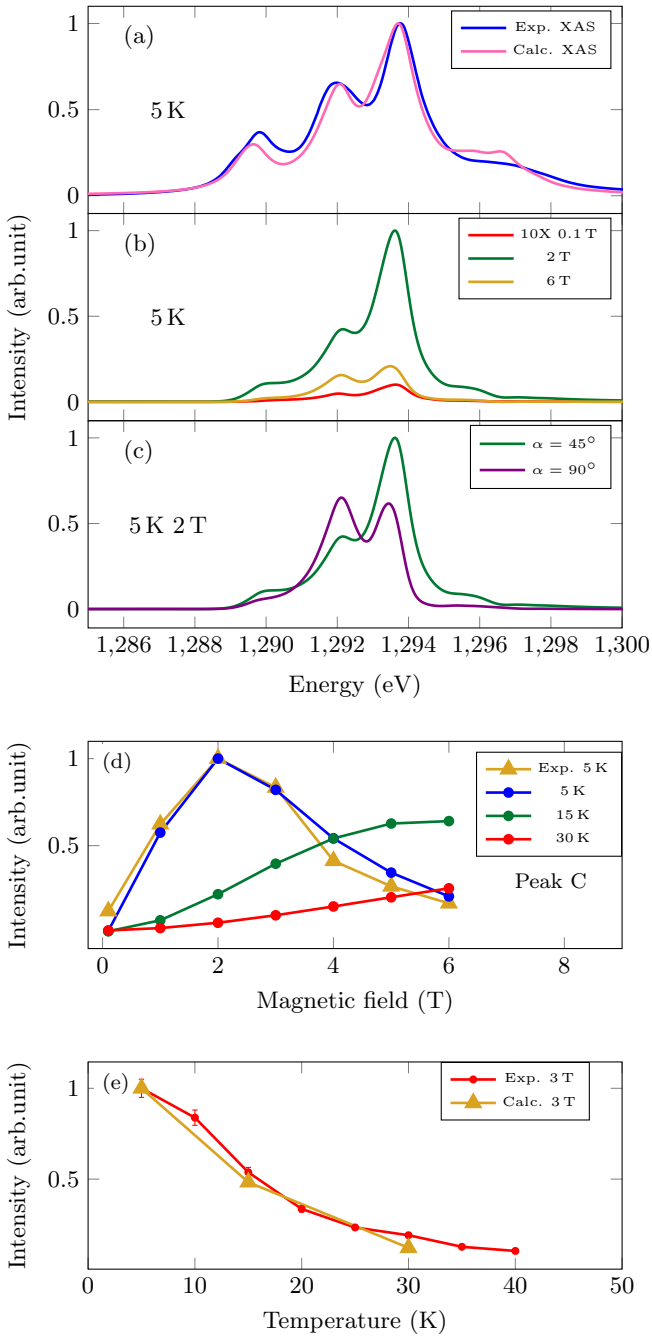

FIG. 10. (a) Comparison between the experimental and calculated XAS spectra. (b) Calculations for the RXS spectral shape at 5 K for three values of magnetic field with $\alpha = 45°$. In (c) we compare the signal for $\alpha = 45°$ and $\alpha = 90°$ (out-of-plane field). (d) Field dependence of the RXS intensity at peak C for increasing temperature. We show the 5 K curve together with the experimental data for the same temperature [Fig. 5(a)]. The experimental data was normalized to the max value, while the other curves have been normalized to the max value of the 5 K one. (e) Temperature dependence of the RXS intensity at peak C at 3 T compared to the experimental data of Fig. 3(a). Both curves have been normalized to 1. See text for details of the calculations.

scattering cross section arises from Dy moments whose magnitudes are modulated at the CDW (or ortho-order) wave vector by the CDW (or ortho-order) induced modulations of the crystal field. Pinpointing the specific orientation of the moments is nontrivial. We cannot exclude the presence of anisotropies and of a variety of inequivalent Dy ions, which will possess different magnetic responses. When simply considering the ratio of the charge order signal for the two incoming light polarizations, where the RXS intensity for the two cases is given by $(\vec{\varepsilon}_{\text{in}} \times \vec{\varepsilon}_{\text{out}}) \cdot \vec{M}$, one would conclude that the magnetization $\vec{M}$ is pointing $\sim 20°$ away from the c axis. This would imply that the magnetic moment is not fully aligned along the field but possesses a significant out-of-plane anisotropy. However, the same exercise carried out for the ortho-order scattering geometry would give a different magnetization direction. That is because this approach is oversimplified. The reality is likely more complicated: In particular, the magnetic signal does not necessarily correspond to ferromagnetically ordered/polarized moments. Given the incommensurate wave vector, one would rather first consider an antiferromagnetic modulation, which can be independent of the lattice periodicity and could easily possess moments perpendicular to the ferromagnetic polarization direction set by the external field. This highlights the challenge of providing a definitive answer on the direction of the induced moments. Nevertheless, the clear saturation of the dichroic signal that we observe strongly suggests that we are aligning the induced moments as the field is increased.

The calculated RXS signal is shown in Fig. 10. The spectral shape of the resonance at the different field and temperature values qualitatively reproduces the experimental data for both induced CDW and ortho-order, mimicking field as well as temperature dependencies, with a reasonable, albeit rough, quantitative agreement. In particular, the striking observation of a nonmonotonic field dependence of the RXS intensity is reproduced at low temperatures corresponding to the experimental conditions. Figure 10(b) ($T = 5$ K) clearly shows that the RXS signal at 2 T is significantly higher compared to 0.1 T and 6 T. The complete field dependence shown in Fig. 10(d) for three temperatures is in very good agreement with the experimental data. We interpret this nonmonotonic behavior in terms of two regimes. In the low-field regime the amplitude of the CDW-induced (or ortho-order induced) modulation of the local Dy moments reflects the magnitude of the Dy sublattice magnetization and thus grows with increasing field strength. For higher field strengths the Dy magnetization is essentially saturated. Further increases in the field only serve to bring the states preferred by the Zeeman splitting so far down in energy that the RXS intensity at the CDW (or ortho-order) wave vector is suppressed. This picture is supported by XMCD measurements performed at the Dy M_5 edge (Fig. 9), which demonstrate paramagnetic behavior with saturation at $\sim$ 2-3 T. Our model further captures the dramatic reduction of the RXS intensity for photon energies corresponding to peak C in Fig. 7(a), when the magnetic field is applied along the out-of-plane direction ($\alpha = 90°$) compared to $\alpha = 45°$. This is shown in Fig. 10(c). A complete quantitative agreement with the data would involve the optimization of a great number of model parameters, and would likely be complicated by the presence of disorder in the system. Accordingly, a comprehensive model exceeds the scope of this study and may be the subject of future work.

V. CONCLUSIONS

We have reported RXS measurements of underdoped thin films of the high-temperature superconductor $DyBa_2Cu_3O_{6+x}$ grown on $NdGaO_3$ (110) substrates. The films were found to host both ortho-II oxygen order as well as a 2D CDW, akin to those observed in bulk underdoped YBCO but with shorter correlation lengths. Unlike thin films of YBCO, which were recently reported to host 3D CDW correlations at zero field [12], the CDW observed in our films was found to be only weakly correlated along the c direction. Our central result is the additional observation of both the ortho-II order and the CDW reflections for incident photon energies tuned to the Dy M_5 resonance. The temperature dependence of these diffraction peaks reveals the induced nature of these ordering tendencies, while both the photon energy and magnetic field dependencies indicate a magnetic contribution to the resonant scattering cross section. The magnetic moments of the Dy ions in the "123" cuprate structure can thus be used as a sensitive probe of both structural ordering tendencies, as well as the electronic correlations in the CuO_2 planes. In the related system $PrBa_2Cu_3O_{6+x}$, a complex interaction between the Pr $4f$ moments and the CuO_2 planes has previously been reported [36]. Future studies of the charge ordered state in this nonsuperconducting system may reveal further insights into the role of the $4f$ moments in coupling to both the CDW and superconductivity.

ACKNOWLEDGMENTS

We acknowledge financial support from the Deutsche Forschungsgemeinschaft (DFG, German Research Foundation), Project No. 107745057 TRR 80, the European Union's Horizon 2020 research and innovation programme under Grant Agreement No. 823717- ESTEEM3, and the Alexander von Humboldt Foundation.

[1] B. Keimer, S. A. Kivelson, M. R. Norman, S. Uchida, and J. Zaanen, From quantum matter to high-temperature superconductivity in copper oxides, Nature (London) **518**, 179 (2015).

[2] M. v. Zimmermann, J. R. Schneider, T. Frello, N. H. Andersen, J. Madsen, M. Käll, H. F. Poulsen, R. Liang, P. Dosanjh, and W. N. Hardy, Oxygen-ordering superstructures in underdoped $YBa_2Cu_3O_{6+x}$ studied by hard x-ray diffraction, Phys. Rev. B **68**, 104515 (2003).

[3] G. Ghiringhelli, M. Le Tacon, M. Minola, S. Blanco-Canosa, C. Mazzoli, N. B. Brookes, G. M. De Luca, A. Frano, D. G. Hawthorn, F. He, T. Loew, M. Moretti Sala, D. C. Peets, M. Salluzzo, E. Schierle, R. Sutarto, G. A. Sawatzky, E. Weschke, B. Keimer, and L. Braicovich, Long-range incommensurate charge fluctuations in $(Y,Nd)Ba_2Cu_3O_{6+x}$, Science **337**, 821 (2012).

[4] R. Comin, R. Sutarto, E. H. da Silva Neto, L. Chauviere, R. Liang, W. N. Hardy, D. A. Bonn, F. He, G. A. Sawatzky, and A. Damascelli, Broken translational and rotational symmetry via charge stripe order in underdoped $YBa_2Cu_3O_{6+y}$, Science **347**, 1335 (2015).

[5] H.-H. Kim, E. Lefrançois, K. Kummer, R. Fumagalli, N. B. Brookes, D. Betto, S. Nakata, M. Tortora, J. Porras, T. Loew, M. Barber, L. Braicovich, G. Ghiringhelli, A. P. Mackenzie, C. W. Hicks, B. Keimer, M. Minola, and M. Le Tacon, Charge density waves in $YBa_2Cu_3O_{6.67}$ probed by resonant x-ray scattering under uniaxial compression (unpublished).

[6] J. Chang, E. Blackburn, A. T. Holmes, N. B. Christensen, J. Larsen, J. Mesot, Ruixing Liang, D. A. Bonn, W. N. Hardy, A. Watenphul, M. v. Zimmermann, E. M. Forgan, and S. M. Hayden, Direct observation of competition between superconductivity and charge density wave order in $YBa_2Cu_3O_{6.67}$, Nat. Phys. **8**, 871 (2012).

[7] S. Blanco-Canosa, A. Frano, T. Loew, Y. Lu, J. Porras, G. Ghiringhelli, M. Minola, C. Mazzoli, L. Braicovich, E. Schierle, E. Weschke, M. Le Tacon, and B. Keimer, Momentum-Dependent Charge Correlations in $YBa_2Cu_3O_{6+\delta}$ Superconductors Probed by Resonant X-Ray Scattering: Evidence for Three Competing Phases, Phys. Rev. Lett. **110**, 187001 (2013).

[8] A. Frano, S. Blanco-Canosa, B. Keimer, and R. J Birgeneau, Charge ordering in superconducting copper oxides, J. Phys.: Condens. Matter **32**, 374005 (2020).

[9] S. Gerber, H. Jang, H. Nojiri, S. Matsuzawa, H. Yasumura, D. A. Bonn, R. Liang, W. N. Hardy, Z. Islam, A. Mehta, S. Song, M. Sikorski, D. Stefanescu, Y. Feng, S. A. Kivelson, T. P. Devereaux, Z.-X. Shen, C.-C. Kao, W.-S. Lee, D. Zhu, and J.-S. Lee, Three-dimensional charge density wave order in $YBa_2Cu_3O_{6.67}$ at high magnetic fields, Science **350**, 949 (2015).

[10] J. Chang, E. Blackburn, O. Ivashko, A. T. Holmes, N. B. Christensen, M. Hücker, Ruixing Liang, D. A. Bonn, W. N. Hardy, U. Rütt, M. v. Zimmermann, E. M. Forgan, and S. M. Hayden, Magnetic field controlled charge density wave coupling in underdoped $YBa_2Cu_3O_{6+x}$, Nat. Commun. **7**, 11494 (2016).

[11] H.-H. Kim, S. M. Souliou, M. E. Barber, E. Lefrançois, M. Minola, M. Tortora, R. Heid, N. Nandi, R. A. Borzi, G. Garbarino, A. Bosak, J. Porras, T. Loew, M. König, P. M. Moll, A. P. Mackenzie, B. Keimer, C. W. Hicks, and M. Le Tacon, Uniaxial pressure control of competing orders in a high-temperature superconductor, Science **362**, 1040 (2018).

[12] M. Bluschke, A. Frano, E. Schierle, D. Putzky, F. Ghorbani, R. Ortiz, H. Suzuki, G. Christiani, G. Logvenov, E. Weschke, R. J. Birgeneau, E. H. da Silva Neto, M. Minola, S. Blanco-Canosa, and B. Keimer, Stabilization of three-dimensional charge order in $YBa_2Cu_3O_{6+x}$ via epitaxial growth, Nat. Commun. **9**, 2978 (2018).

[13] M. Bluschke, M. Yaari, E. Schierle, G. Bazalitsky, J. Werner, E. Weschke, and A. Keren, Adiabatic variation of the charge density wave phase diagram in the 123 cuprate $(Ca_xLa_{1-x})(Ba_{1.75-x}La_{0.25+x})Cu_3O_y$, Phys. Rev. B **100**, 035129 (2019).

[14] J. P. Hill, D. F. McMorrow, A. T. Boothroyd, A. Stunault, C. Vettier, L. E. Berman, M. v. Zimmermann, and Th. Wolf, X-ray-scattering study of copper magnetism in nonsuperconducting $PrBa_2Cu_3O_{6.92}$, Phys. Rev. B **61**, 1251 (2000).

[15] D. Putzky, P. Radhakrishnan, Y. Wang, P. Wochner, G. Christiani, M. Minola, P. A. van Aken, G. Logvenov,

E. Benckiser, and B. Keimer, Strain-induced structural transition in $DyBa_2Cu_3O_{7-x}$ films grown by atomic layer-by-layer molecular beam epitaxy, Appl. Phys. Lett. **117**, 072601 (2020).

[16] V. Likodimos, N. Guskos, J. Typek, and M. Wabia, EPR study of Dy^{3+} ions in $DyBa_2Cu_3O_{6+x}$, Eur. Phys. J. B **24**, 143 (2001).

[17] P. Allenspach, A. Furrer, and F. Hulliger, Neutron crystal-field spectroscopy and magnetic properties of $DyBa_2Cu_3O_{7-\delta}$, Phys. Rev. B **39**, 2226 (1989).

[18] A. I. Goldman, B. X. Yang, J. Tranquada, J. E. Crow, and Chan-Soo Jee, Antiferromagnetic order in $DyBa_2Cu_3O_7$, Phys. Rev. B **36**, 7234 (1987).

[19] P. Allenspach, A. Furrer, B. Rupp, and H. Blank, Oxygen-vacancy induced changes of the crystal-field interaction in $ErBa_2Cu_3O_x (6.1 \leqslant x \leqslant 7.0)$ determined by inelastic neutron scattering, Physica C: Superconductivity **161**, 671 (1989).

[20] S. Blanco-Canosa, A. Frano, E. Schierle, J. Porras, T. Loew, M. Minola, M. Bluschke, E. Weschke, B. Keimer, and M. Le Tacon, Resonant x-ray scattering study of charge-density wave correlations in $YBa_2Cu_3O_{6+x}$, Phys. Rev. B **90**, 054513 (2014).

[21] T. Steinborn, G. Miehe, J. Wiesner, E. Brecht, H. Fuess, G. Wirth, B. Schulte, M. Speckmann, H. Adrian, M. Maul, K. Petersen, W. Blau, and M. McConnel, Twinning of $YBa_2Cu_3O_7$ thin films on different substrates and modification by irradiation, Physica C: Superconductivity **220**, 219 (1994).

[22] See Supplemental Material at http://link.aps.org/supplemental/10.1103/PhysRevB.102.195149 for details about sample degradation, the 2D nature of the CDW, additional data and comparison with the calculations.

[23] D. G. Hawthorn, K. M. Shen, J. Geck, D. C. Peets, H. Wadati, J. Okamoto, S.-W. Huang, D. J. Huang, H.-J. Lin, J. D. Denlinger, Ruixing Liang, D. A. Bonn, W. N. Hardy, and G. A. Sawatzky, Resonant elastic soft x-ray scattering in oxygen-ordered $YBa_2Cu_3O_{6+\delta}$, Phys. Rev. B **84**, 075125 (2011).

[24] E. Schierle, V. Soltwisch, D. Schmitz, R. Feyerherm, A. Maljuk, F. Yokaichiya, D. N. Argyriou, and E. Weschke, Cycloidal Order of $4f$ Moments as A Probe of Chiral Domains in $DyMnO_3$, Phys. Rev. Lett. **105**, 167207 (2010).

[25] H. Ott, C. Schüßler-Langeheine, E. Schierle, A. Yu. Grigoriev, V. Leiner, H. Zabel, G. Kaindl, and E. Weschke, Magnetic x-ray scattering at the M_5 absorption edge of Ho, Phys. Rev. B **74**, 094412 (2006).

[26] Specifically, all three peaks (A,B,C) can be related to magnetic transitions but, while peaks A and C are of circular dichroic nature and lead to magnetic scattering peaks, peak B plays the dominant role for linear dichroic effects responsible for orbital ordering or second-order magnetic peaks.

[27] O. Prokhnenko, R. Feyerherm, E. Dudzik, S. Landsgesell, N. Aliouane, L. C. Chapon, and D. N. Argyriou, Enhanced Ferroelectric Polarization by Induced dy Spin Order in Multiferroic $DyMnO_3$, Phys. Rev. Lett. **98**, 057206 (2007).

[28] C. Donnerer, M. C. Rahn, E. Schierle, R. S. Perry, L. S. I. Veiga, G. Nisbet, S. P. Collins, D. Prabhakaran, A. T. Boothroyd, and D. F. McMorrow, Selective probing of magnetic order on Tb and Ir sites in stuffed $Tb_2Ir_2O_7$ using resonant x-ray scattering, J. Phys.: Condens. Matter **31**, 344001 (2019).

[29] W. S. Lee, A. P. Sorini, M. Yi, Y. D. Chuang, B. Moritz, W. L. Yang, J.-H. Chu, H. H. Kuo, A. G. Cruz Gonzalez, I. R. Fisher, Z. Hussain, T. P. Devereaux, and Z. X. Shen, Resonant enhancement of charge density wave diffraction in the rare-earth tritellurides, Phys. Rev. B **85**, 155142 (2012).

[30] M. Bluschke, A. Frano, E. Schierle, M. Minola, M. Hepting, G. Christiani, G. Logvenov, E. Weschke, E. Benckiser, and B. Keimer, Transfer of Magnetic Order and Anisotropy Through Epitaxial Integration of $3d$ and $4f$ Spin Systems, Phys. Rev. Lett. **118**, 207203 (2017).

[31] Strictly speaking, DyBCO is not magnetically ordered at zero field, so that the transitions at peak A and C do not mainly correspond to single ΔM_J transitions. However, by applying an external field, we bring the system closer to this approximation. The magnetic origin of the RXS intensity excited at peak C is clear anyway from the strong field dependence.

[32] M. W. Haverkort, M. Zwierzycki, and O. K. Andersen, Multiplet ligand-field theory using Wannier orbitals, Phys. Rev. B **85**, 165113 (2012).

[33] Robert D Cowan, *The Theory of Atomic Structure and Spectra* (University of California Press, Berkeley, 1981).

[34] Note that RXS is sensitive only to the difference in the scattering tensors of the two ions, while inelastic neutron scattering is a direct probe of the CF splitting. In addition, the crystal field in thin-film structure may differ from the bulk, especially for ions near the surface and substrate interface.

[35] M. W. Haverkort, N. Hollmann, I. P. Krug, and A. Tanaka, Symmetry analysis of magneto-optical effects: The case of x-ray diffraction and x-ray absorption at the transition metal $L_{2,3}$ edge, Phys. Rev. B **82**, 094403 (2010).

[36] J. P. Hill, A. T. Boothroyd, N. H. Andersen, E. Brecht, and Th. Wolf, Incommensurate magnetism in $PrBa_2Cu_3O_{6.92}$, Phys. Rev. B **58**, 11211 (1998).